

Supramolecular “Trojan Horse” for Nuclear Delivery of Dual Anticancer Drugs

Yanbin Cai,[†] Haosheng Shen,[†] Jie Zhan,[†] Mingliang Lin,[†] Liuhan Dai,[†] Chunhua Ren,[‡] Yang Shi,[†] Jianfeng Liu,^{*,‡} Jie Gao,^{*,†} and Zhimou Yang^{*,†}

[†]State Key Laboratory of Medicinal Chemical Biology, Key Laboratory of Bioactive Materials, Ministry of Education, College of Life Sciences, and Collaborative Innovation Center of Chemical Science and Engineering (Tianjin), Nankai University, Tianjin 300071, P. R. China

[‡]Tianjin Key Laboratory of Radiation Medicine and Molecular Nuclear Medicine, Institute of Radiation Medicine, Chinese Academy of Medical Science and Peking Union Medical College, Tianjin 300192, P. R. China

S Supporting Information

ABSTRACT: Nuclear delivery and accumulation are very important for many anticancer drugs that interact with DNA or its associated enzymes in the nucleus. However, it is very difficult for neutrally and negatively charged anticancer drugs such as 10-hydroxycamptothecin (HCPT). Here we report a simple strategy to construct supramolecular nanomedicines for nuclear delivery of dual synergistic anticancer drugs. Our strategy utilizes the coassembly of a negatively charged HCPT-peptide amphiphile and the positively charged cisplatin. The resulting nanomaterials behave as the “Trojan Horse” that transported soldiers (anticancer drugs) across the walls of the castle (cell and nucleus membranes). Therefore, they show improved inhibition capacity to cancer cells including the drug resistant cancer cell and promote the synergistic tumor suppression property in vivo. We envision that our strategy of constructing nanomaterials by metal chelation would offer new opportunities to develop nanomedicines for combination chemotherapy.

Traditional chemotherapy is often associated with severe side effects from the systemic toxicity of anticancer drugs and undesired drug resistance of cancer cells.¹ To address these problems, nanomedicines have been extensively explored to reduce the systemic toxicity of anticancer drugs by targeting delivery of them to tumors.^{2–5} Besides, combinatorial drug therapy has also been widely applied to provide a synergistic therapeutic effect to overcome drug resistance.⁶ Therefore, nanomedicine capable of simultaneously delivering multiple therapeutic molecules attracts significant research interests recently, because of its lower toxicity and improved efficacy.^{7–10} However, most of the nanocarriers developed to date can only deliver multiple drugs into cells rather than subcellular organelles. Many first-line anticancer drugs interact with DNA or its associated enzymes within the nucleus. For instance, doxorubicin and cisplatin chelate with DNA molecules and camptothecin inhibits DNA enzyme topoisomerase I.^{11–13} Thus, it is very important to develop nanomedicines with nuclear delivery and the accumulation effects of multiple anticancer drugs.^{14–17}

Recently, a novel kind of drug delivery system based on supramolecular self-assembly of drug amphiphiles has been reported.^{18–22} The drug amphiphiles spontaneously self-assemble into nanomaterials that serve as both carriers and cargos. Compared with other drug delivery systems with physically encapsulated therapeutics, such nanomaterials exhibit much higher drug loadings and constant drug release capacities.^{20,23} Moreover, the drug loading in this system can be controlled by the variation of weight ratio of drug molecule. Up to now, self-assembling drug amphiphiles based on anticancer^{23–25} and anti-inflammatory²⁶ therapeutics have been reported, and nanomedicines utilizing them show improved efficacy or reduced side effects. However, to the best of our knowledge, none of these drug delivery systems shows efficient nuclear delivery capacity. In this study, we report supramolecular nanomedicines with an efficient nuclear accumulation effect for dual anticancer drugs (Figure 1A).

We choose 10-hydroxycamptothecin (HCPT) and cisplatin to construct the dual anticancer drugs assemblies because (i) HCPT was the DNA-topoisomerase I inhibitor and cisplatin inhibited the DNA synthesis by interacting with DNA, and synergistic effects were observed when topoisomerase I inhibitors were combined with cisplatin in several tumor cells;^{27,28} (ii) they had no overlapping toxicity profiles;^{6,10} and (iii) HCPT encountered difficulty entering the nucleus, while cisplatin might assist the dual-drug assemblies entering into the nucleus because of its positive charge, just like the nuclear localizing properties of cationic polymers.²⁹ We designed an HCPT-peptide (*HP*) amphiphile of HCPT-FFERGD (Figure 1B). The cisplatin and other platinum(II)-based drugs had been widely reported to be able to form complexes with biopolymers and peptides containing carboxylic acid groups.^{30,31} We and other groups had also demonstrated that dipeptide FF, and its derivatives possessed excellent self-assembling properties.^{24,32–34} We therefore imagined that *HP* might chelate with cisplatin and self-assemble into certain kinds of nanostructures.

The *HP* was synthesized by first reacting HCPT with glutaric anhydride, and then conjugating to the peptide FFERGD in

Received: November 29, 2016

Published: February 13, 2017

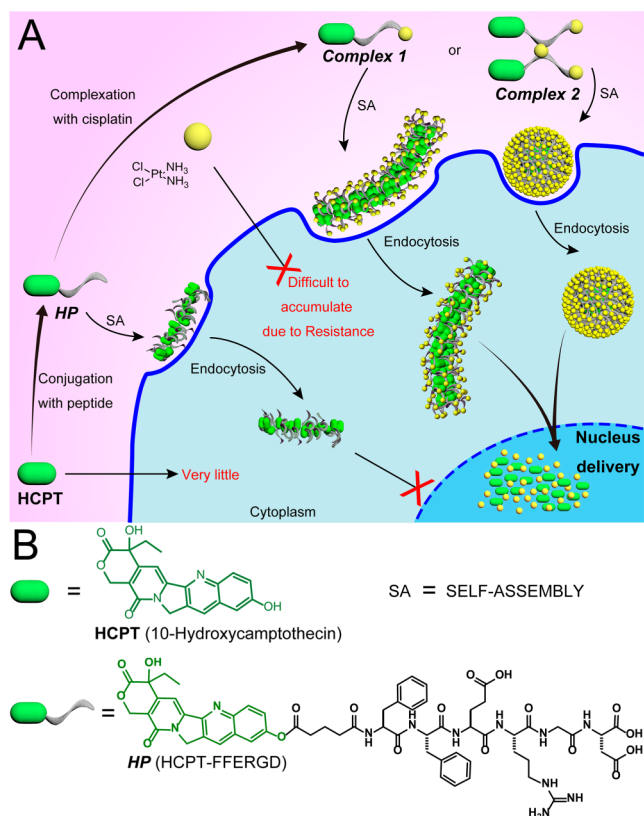


Figure 1. (A) Schematic illustration for preparation of dual-drug assemblies and the nuclear drug delivery. (B) Chemical structures of HCPT and HP.

DMSO, followed by purification via reversed-phase high performance liquid chromatography. The HP formed stable clear solutions in water at the concentration 1 mg/mL (pH = 7.4, Figure S10A) in the absence or in the presence of 1.0 or 1.5 equiv of cisplatin (Figure S10B and S10C). However, it formed precipitates in the presence of 2 and 5 equiv of cisplatin (Figure S10D and S10E). The transmission electron microscopy (TEM) images in Figure 2A revealed that HP formed short nanofibers with a diameter of 6–9 nm and a length of less than

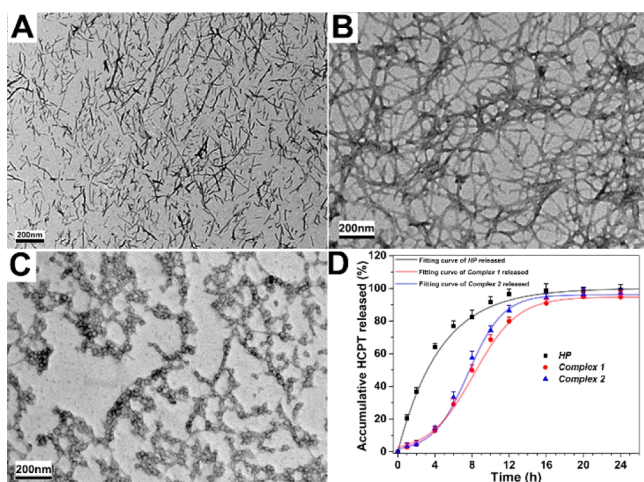


Figure 2. TEM image of solution containing 100 μM of (A) HP, (B) Complex 1, and (C) Complex 2, and (D) accumulative release profile from solution containing 1 mg/mL of different compounds.

1 μm. In the presence of 1 equiv of cisplatin, HP interacted with cisplatin to form Complex 1, which self-assembled into long nanofibers with a width of 10–15 nm (Figure 2B). Complex 2 with 1.5 equiv of cisplatin formed nanoparticles with a diameter of 20–25 nm (Figures 2C and S12). ¹H NMR spectra (Figure S11) confirmed that cisplatin in both complexes chelated with carboxylic acids on HP. The critical micelle concentration (CMC) of Complex 1 and Complex 2 was 22.8 and 29.3 μM, respectively, which was about four times lower than that of HP (85.5 μM, Figure S13). These observations clearly indicated that cisplatin could chelate with the drug–peptide amphiphile, thus increasing its self-assembly property. Both analogues of HP (HCPT-FFARGD and HCPT-FFERGA) with more hydrophobic amino acids instantly aggregated into precipitates in the presence of 1 equiv of cisplatin (Figure S9), suggesting the importance of balance between hydrophobicity and -philicity in the formation of stable nanostructures.

The release profiles of HCPT from nanomaterials were then assessed at 37 °C by LC-MS (Figure 2D). The results clearly showed that, in the first 4 h, only less than 15% of HCPT got released from both complexes, while 64% of HCPT was already released. The slower releasing speed from the complexes than that from HP was probably due to the enhanced self-assembling properties of the complexes. It was worth noting that the release of HCPT raised rapidly from 4 to 16 h. The latter burst release of HCPT from both complexes was due the release of cisplatin. There were less than 10% of cisplatin got released from both complexes in the first 4 h, and about 90% of cisplatin got released in the following 12 h. After losing more and more amounts of cisplatin, the nanostructures of both complexes dissociated, thus making the release of HCPT faster.

In order to see whether the internalization of drugs will be improved by the formation of nanomaterials, we used a cisplatin-resistant cell line, A549/DDP, to perform the cellular uptake experiments. The results in Figure 3A and 3B indicated that, at each time point, the intracellular concentration of HCPT in cells treated with both complexes was higher than that treated with free HCPT and HP. The amount of Pt in A549/DDP cells was also evaluated by ICP-AES (Figure 3B). Because of the resistance to cisplatin, the accumulation of Pt in cisplatin treated cells increased very little from 1 to 4 h (<2 (ng Pt)/(mg protein)). However, the amounts of Pt in cells treated with both complexes continued to increase over 4 h. At the 4 h time point, Complex 1 and Complex 2 had about 232 and 242 times higher Pt accumulation in cells compared to those treated with cisplatin, reaching 464 and 484 (ng Pt)/(mg protein), respectively. These observations clearly indicated that the cellular uptake of both HCPT and cisplatin was significantly improved by nanostructure formation.

A much lower cellular uptake of Complex 1 and Complex 2 was observed at 4 °C than that at 37 °C, but for HP there was no such difference (Figure S15), suggesting that the uptake of nanostructures formed by Complex 1 and 2 was due to endocytosis, because all endocytic pathways were energy-dependent processes that would slow down at low temperatures. To determine the possible pathways of endocytotic process, we used several endocytotic inhibitors (chlorpromazine (CPZ), 5-(N-ethyl-N-isopropyl)-amiloride (EIPA), and Filipin III for clathrin, micropinocytosis, and caveolae-mediated endocytosis, respectively) with Complexes 1 and 2 to treat A549 cells. As shown in Figure S16, addition of CPZ or EIPA

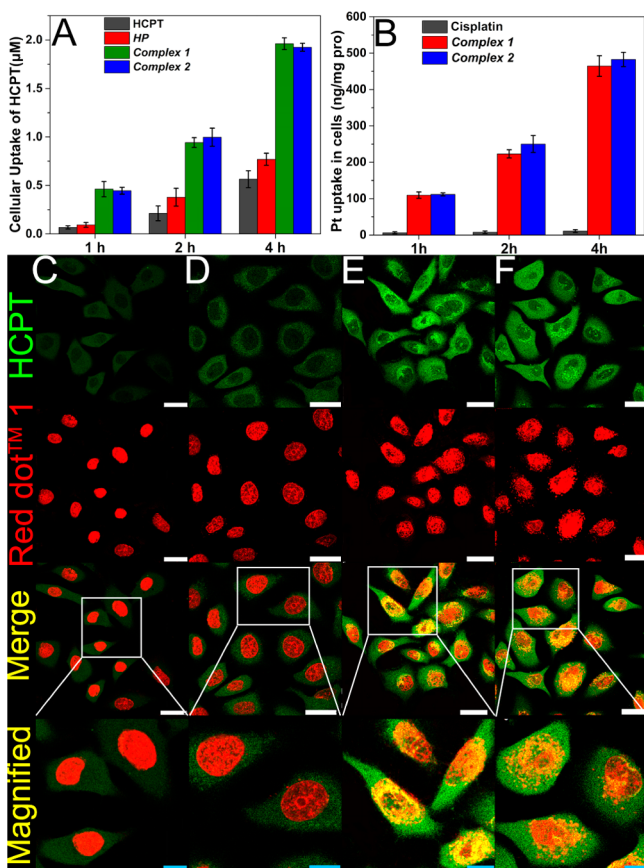


Figure 3. Intracellular concentration of (A) HCPT and (B) Pt in A549 cells (SEM \pm mean, $n = 3$), CLSM images of A549 cells treated with (C) HCPT, (D) *HP*, (E) *Complex 1*, and (F) *Complex 2* (100 μ M) for 2 h, and then stained with 1 \times Red dot 1. Scale bar represent 25 and 10 μ m at low and high magnification images, respectively.

hardly affected the uptake of both complexes, while the addition of Filipin III significantly reduced the uptake of *Complex 1* and *2* for about 94% and 93%, respectively. These results suggested that the internalization of nanostructures mainly underwent caveolae-mediated endocytosis.

We also investigated the subcellular localization of HCPT in A549 cells via confocal laser scanning microscopy (CLSM). As shown in Figure S17, weak green fluorescence from HCPT was observed from the cytoplasm of cells treated with HCPT and *HP* at the 2 h time point. However, cells treated with both complexes showed much stronger green fluorescence which overlapped well with the red fluorescence from lysotacker, further indicating that nanostructures of both complexes entered the cells via endocytosis. We surprisingly observed obvious green fluorescence in the nucleus of cells treated with both complexes (Figure 3E and 3F) but not in those treated with HCPT and *HP* (Figure 3C and 3D), which was demonstrated by the results that the green fluorescence from HCPT was not only in the cytoplasm but also in nucleus overlapping with the red fluorescence of Red dot 1. The ζ -potential of nanostructures formed by *HP*, *Complex 1*, and *Complex 2* was -38.0 , 9.8 , and 14.4 mV, respectively (Figure S14). We therefore concluded that the nuclear accumulation of HCPT in cells treated with both complexes was due to the formation of positively charged nanomaterials. These observations suggested that the role of nanostructures of both complexes was analogous to that of the “Trojan Horse”

which hid and transported soldiers (anticancer drugs) across the walls of the castle (cell and nucleus membranes). The nuclear accumulation of HCPT would be crucial to the anticancer property of nanomedicines.

Our supramolecular “Trojan Horse” formed by either complex had a higher cytotoxic effect than free HCPT or cisplatin (Figure 4A) to cancer cells. Especially for A549/DDP

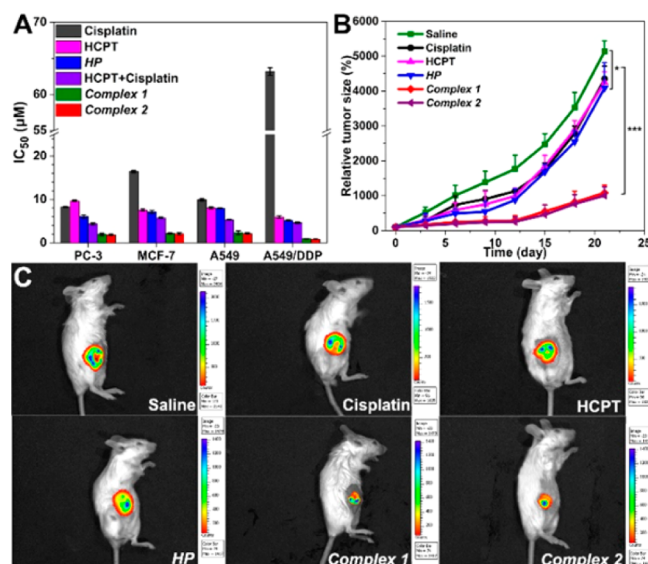


Figure 4. (A) IC_{50} value, (B) *in vivo* anticancer efficacy, and (C) bioluminescent imaging of tumors at 22 d in mice with the treatment of different drugs.

cells, *Complex 1* and *Complex 2* had a 69.4 and 75.4 times higher cytotoxicity than free cisplatin, respectively. The IC_{50} value of both complexes to cancer cells was below 5 μ M, which was much lower than their CMC value. The results of isothermal titration calorimetry (ITC) indicated that *HP* still could bind to cisplatin at the concentration of 2 μ M (Figure S19), suggesting that the two anticancer drugs could be simultaneously taken up by cells. We also observed some green fluorescent dots at the surface of cells (Figure S20) treated with 2 μ M of the complex, which probably formed by surface-induced self-assembly. Surface-induced self-assembly has been demonstrated to be a powerful strategy to form nanomaterials at desired surfaces at a much lower concentration than the critical self-assembly concentration.^{35,36} A combination index (CI) value smaller than 1.0 indicated the synergistic effect, and one bigger than 1.0 indicated an antagonistic or additive effect of two drugs. The CI value of *Complex 1* was 0.44, 0.42, 0.52, and 0.17 and that of *Complex 2* was 0.42, 0.41, 0.48, and 0.16 to PC-3, MCF-7, A549, and A549/DDP cell, respectively. The results clearly indicated the synergistic effect of dual drugs to inhibit cancer cells. In contrast, we only observed antagonistic, additive, or little synergistic effect of HCPT and cisplatin when they were used simultaneously (Figure S21).

The tumor inhibition capacity of different drugs *in vivo* was also evaluated (4T1-luciferase breast tumors in mice; the IC_{50} value against 4T1 cells was shown in Figure S22). As shown in Figures 4B and S23, all drugs exhibited good antitumor efficacy compared with the saline control, and both complexes showed the best efficacy among all drugs. The final volume of tumors at day 21 was 5136%, 4148%, 4251%, 4188%, 982%, and 1005% for the saline control group, cisplatin, HCPT, *HP*, *Complex 1*,

and **Complex 2**, respectively. The body weight loss of mice was observed in groups receiving drugs containing platinum (**Figure S24**), resulting from the toxicity of cisplatin. After drug withdrawal, the body weight of mice rebounded. The *in vivo* images of tumors (**Figure 4C**) indicated that mice that received both complexes showed the smallest size of light spots, which correlated well with the results of tumor volumes obtained in **Figure 4B**. These results clearly indicated that our “Trojan Horse” had excellent capacity to synergistically inhibit tumor growth.

In summary, we prepared supramolecular nanostructures of dual anticancer drugs with synergistic effects. The resulting supramolecular “Trojan Horse” could deliver the two drugs more efficiently to cells, especially to the targeted organelle of the cell nucleus. Thus, our “Trojan Horse” efficiently inhibited cancer cells including a drug resistant one both *in vitro* and *in vivo*. We envision that our strategy may be applied to construct other nanomedicines with metal-based anticancer drugs, which will provide opportunities to develop nucleus localized nanomaterials for combination chemotherapy.

■ ASSOCIATED CONTENT

📄 Supporting Information

The Supporting Information is available free of charge on the ACS Publications website at DOI: 10.1021/jacs.6b12322.

General methods; characterization; dynamic light scattering; emission spectra; confocal images; and details in cell assays (PDF)

■ AUTHOR INFORMATION

Corresponding Authors

*liujianfeng@irm-cams.ac.cn

*chemgaojie@nankai.edu.cn

*yangzm@nankai.edu.cn

ORCID

Jie Gao: 0000-0002-6186-2750

Zhimou Yang: 0000-0003-2967-6920

Notes

The authors declare no competing financial interest.

■ ACKNOWLEDGMENTS

This work is supported by the International S&T Cooperation Program of China (2015DFA50310), NSFC (51403105), Program for Changjiang Scholars and Innovative Research Team in University (IRT13023), and Science & Technology Projects of Tianjin of China (15JCQNJC14300)

■ REFERENCES

- (1) Holohan, C.; Van Schaeybroeck, S.; Longley, D. B.; Johnston, P. *G. Nat. Rev. Cancer* **2013**, *13*, 714.
- (2) Wang, Y.; Brown, P.; Xia, Y. *Nat. Mater.* **2011**, *10*, 482.
- (3) Jain, R. K.; Stylianopoulos, T. *Nat. Rev. Clin. Oncol.* **2010**, *7*, 653.
- (4) Davis, M. E.; Chen, Z.; Shin, D. M. *Nat. Rev. Drug Discovery* **2008**, *7*, 771.
- (5) Peer, D.; Karp, J. M.; Hong, S.; Farokhzad, O. C.; Margalit, R.; Langer, R. *Nat. Nanotechnol.* **2007**, *2*, 751.
- (6) Al-Lazikani, B.; Banerji, U.; Workman, P. *Nat. Biotechnol.* **2012**, *30*, 679.
- (7) Goldman, A.; Kulkarni, A.; Kohandel, M.; Pandey, P.; Rao, P.; Natarajan, S. K.; Sabbisetti, V.; Sengupta, S. *ACS Nano* **2016**, *10*, 5823.
- (8) Kemp, J. A.; Shim, M. S.; Heo, C. Y.; Kwon, Y. J. *Adv. Drug Delivery Rev.* **2016**, *98*, 3.

- (9) Zhao, Y. Y.; Chen, F.; Pan, Y. M.; Li, Z. P.; Xue, X. D.; Okeke, C. I.; Wang, Y. F.; Li, C.; Peng, L.; Wang, P. C.; Ma, X. W.; Liang, X. J. *ACS Appl. Mater. Interfaces* **2015**, *7*, 19295.
- (10) Liao, L. Y.; Liu, J.; Dreaden, E. C.; Morton, S. W.; Shopsowitz, K. E.; Hammond, P. T.; Johnson, J. A. *J. Am. Chem. Soc.* **2014**, *136*, 5896.
- (11) Wang, D.; Lippard, S. J. *Nat. Rev. Drug Discovery* **2005**, *4*, 307.
- (12) Pommier, Y. *Nat. Rev. Cancer* **2006**, *6*, 789.
- (13) Hurley, L. H. *Nat. Rev. Cancer* **2002**, *2*, 188.
- (14) Biswas, S.; Torchilin, V. P. *Adv. Drug Delivery Rev.* **2014**, *66*, 26.
- (15) Pan, L. M.; Liu, J. N.; He, Q. J.; Shi, J. L. *Adv. Mater.* **2014**, *26*, 6742.
- (16) Sui, M. H.; Liu, W. W.; Shen, Y. Q. *J. Controlled Release* **2011**, *155*, 227.
- (17) Kang, B.; Mackey, M. A.; El-Sayed, M. A. *J. Am. Chem. Soc.* **2010**, *132*, 1517.
- (18) Wang, H.; Feng, Z.; Wu, D.; Fritzsche, K. J.; Rigney, M.; Zhou, J.; Jiang, Y.; Schmidt-Rohr, K.; Xu, B. *J. Am. Chem. Soc.* **2016**, *138*, 10758.
- (19) Huang, P.; Wang, D.; Su, Y.; Huang, W.; Zhou, Y.; Cui, D.; Zhu, X.; Yan, D. *J. Am. Chem. Soc.* **2014**, *136*, 11748.
- (20) Cheetham, A. G.; Zhang, P. C.; Lin, Y. A.; Lock, L. L.; Cui, H. *G. J. Am. Chem. Soc.* **2013**, *135*, 2907.
- (21) Shen, Y.; Jin, E.; Zhang, B.; Murphy, C. J.; Sui, M.; Zhao, J.; Wang, J.; Tang, J.; Fan, M.; Van Kirk, E.; Murdoch, W. J. *J. Am. Chem. Soc.* **2010**, *132*, 4259.
- (22) Webber, M. J.; Matson, J. B.; Tamboli, V. K.; Stupp, S. I. *Biomaterials* **2012**, *33*, 6823.
- (23) Wang, H.; Wei, J.; Yang, C.; Zhao, H.; Li, D.; Yin, Z.; Yang, Z. *Biomaterials* **2012**, *33*, 5848.
- (24) Gao, Y.; Kuang, Y.; Guo, Z.-F.; Guo, Z.; Krauss, I. J.; Xu, B. *J. Am. Chem. Soc.* **2009**, *131*, 13576.
- (25) Su, H.; Koo, J. M.; Cui, H. *J. Controlled Release* **2015**, *219*, 383.
- (26) Pappas, C. G.; Shafi, R.; Sasselli, I. R.; Siccardi, H.; Wang, T.; Narang, V.; Abzalimov, R.; Wijerathne, N.; Ulijn, R. V. *Nat. Nanotechnol.* **2016**, *11*, 960.
- (27) Souglakos, J.; Syrigos, K.; Potamianou, A.; Polyzos, A.; Boukovinas, I.; Androulakis, N.; Kouroussis, C.; Vardakis, N.; Christophilakis, C.; Kotsakis, A.; Georgoulas, V. *Ann. Oncol.* **2004**, *15*, 1204.
- (28) Zeghari-Squalli, N.; Raymond, E.; Cvitkovic, E.; Goldwasser, F. *C. Cancer Res.* **1999**, *5*, 1189.
- (29) Cortez, M. A.; Godbey, W. T.; Fang, Y. L.; Payne, M. E.; Cafferty, B. J.; Kosakowska, K. A.; Grayson, S. M. *J. Am. Chem. Soc.* **2015**, *137*, 6541.
- (30) Xiao, H.; Song, H.; Zhang, Y.; Qi, R.; Wang, R.; Xie, Z.; Huang, Y.; Li, Y.; Wu, Y.; Jing, X. *Biomaterials* **2012**, *33*, 8657.
- (31) Tseng, C. L.; Su, W. Y.; Yen, K. C.; Yang, K. C.; Lin, F. H. *Biomaterials* **2009**, *30*, 3476.
- (32) Wang, H.; Yang, C.; Tan, M.; Wang, L.; Kong, D.; Yang, Z. *Soft Matter* **2011**, *7*, 3897.
- (33) Reches, M.; Gazit, E. *Science* **2003**, *300*, 625.
- (34) Reches, M.; Gazit, E. *Nat. Nanotechnol.* **2006**, *1*, 195.
- (35) Xu, T.; Liang, C.; Ji, S.; Ding, D.; Kong, D.; Wang, L.; Yang, Z. *Anal. Chem.* **2016**, *88*, 7318.
- (36) Bieser, A. M.; Tiller, J. C. *Chem. Commun.* **2005**, 3942.